Hindawi
Advances in Civil Engineering
Volume 2020, Article ID 9403968, 10 pages
https://doi.org/10.1155/2020/9403968

Research Article

Experimental Study on Seepage Properties of Jointed Rock-Like Samples Based on 3D Printing Techniques

Wenhui Tan[1,2] **and Pengfei Wang**[1,2]

[1]*School of Civil and Resource Engineering, University of Science and Technology Beijing, Beijing 100083, China*
[2]*Beijing Key Laboratory of Urban Underground Space Engineering, University of Science and Technology Beijing, Beijing 100083, China*

Correspondence should be addressed to Wenhui Tan; wenhui.t@ustb.edu.cn

Received 20 September 2019; Revised 29 November 2019; Accepted 10 December 2019; Published 21 January 2020

Guest Editor: Michele Palermo

Sample making of fractured rock mass is a big problem in rock mechanical test. The specimens prepared by traditional rock core drilling have some disadvantages such as unclear internal structure and great difference in mechanical properties; while, the samples prepared by inserting and seaming method have some other disadvantages such as hard to control the attitude of precast-joints, low accuracy. A method for preparing fractured rock-like samples based on 3D printing technology is introduced in this paper, and the seepage characteristics of fractured rock-like samples is studied by seepage experiments. Firstly, the standard profile curves of 10 grades of joint roughness are digitized and 10 groups of 3D digital fracture models are established with different roughness and thickness (i.e., 1.5, 3.0, and 5.0 mm, respectively). 30 fracture inserts are produced by 3D printing technology. Then, rock-like specimens with through-filling fractures are poured with molds. Finally, the permeability tests of the prepared rock-like specimens are carried out to study the seepage characteristics of fractures with different roughness and gap widths under different confining pressures. The results show that 3D printing technology provides an effective way for production of complex crack samples in laboratory test and the comparative analysis of tests. The seepage characteristics of fractures are well studied. When the gap width is small, the permeability decreases with the increase of roughness, and the influence of roughness on fracture permeability decreases rapidly with the increase of confining pressure and gap width. The permeability of through-filling fractures with different roughness and gap width decreases with the increase of confining pressure. The relationship between confining pressure and fracture permeability can be described by the power function. 3D printing technology overcomes the shortcomings of traditional specimen preparation methods and greatly improves the precision of crack inserts. The jointed rock-like model established by the method revealed the influence of fracture characteristics on seepage flow very well.

1. Introduction

Seepage properties of jointed rock mass have great influence on the stabilities of rock engineering; therefore, the study of seepage has always been a hotspot in the field of rock mechanics. Since the 1960s, Snow [1, 2] and Romn [3] carried out the water flow test of parallel plate crack for the first time and proposed the famous cubic law; researchers have done a lot of research on the seepage characteristics of fractured rock mass. Considering the influence of rough fracture surface from different perspectives, Lomize et al. [4–7] introduced roughness influence coefficients into cubic law to analyze the seepage characteristics of rough fracture. Zhu and Wong [8], Han et al. [9], Schulze et al. [10], Oda et al. [11], and Wang and Park [12] preliminarily established the relationship between damage, volume expansion, porosity, and permeability based on different rock mass. Yang et al. [13, 14] obtained the result that the roughness of fracture is an important factor affecting fracture seepage by experiment and the recovery of fracture hydraulic opening has obvious lag phenomenon. Duan et al. [15] studied the tensile fracture surfaces of JRC curve with different roughness coefficients of joints experimentally and obtained the result that the higher the roughness, the lower the

permeability. Zimmerman et al. [16] found the phenomenon of Forchheimer flow in rough fracture when the Reynolds number is bigger than 20 for the first time by means of experiments and numerical method. Zoorabadi et al. [17] carried out saturated seepage test on crack specimens with different roughness coefficients JRC and discussed the effects of Reynolds number and relative roughness on nonlinear seepage characteristics. With the rapid development of computer technology, the numerical simulation method has played an important role in considering the geometrical features of fracture surface and studying the seepage of jointed rock mass. Zhou et al. [18] analyzed the seepage law of rough fracture by the finite element method. Liu et al. [19–23] carried out experimental study and theoretical analysis of seepage characteristics on the basis of discrete fracture network (DFN); they found that the roughness has a big influence on the seepage characteristic of rock mass. Min et al. [24] studied the permeability characterization of representative element volume (REV) of rock mass by the DFN method. Baghbanan et al. [25] studied the influence of opening and trace length of joints on the permeability tensor and analyzed the anisotropy of permeability.

Single fracture is the basic element of fracture network; the seepage property of a single fracture has also been studied, for example, Wang et al. [26, 27] and Xiong et al. [28] studied the two basic parameters describing geometric characteristics of single fracture surface, gap width and roughness, and discussed the way of determination of fractures with different roughness and the equivalent hydraulic gap width. He et al. [29] prepared ten cylindrical cement samples with single fracture and different JRCs and carried out seepage tests; they found JRC has a great influence on seepage characteristics of single fracture at low stress, and on the contrary, the influence decreases rapidly.

The gap width and roughness of fracture have a great influence on macroscopic mechanical properties of jointed rock masses, but there are relatively few studies on the mechanical properties of jointed rock masses considering the roughness and gap width under different confining pressures. The mechanism of roughness and gap width on the mechanical properties of jointed rock masses is also not well recognized, so it is necessary to study the influence of roughness and gap width by test.

Laboratory tests can simulate the stress and deformation characteristics of rock mass comprehensively and truly, which is one of the important means to study the characteristics of engineering rock mass. In the process of numerical simulation, the structure of complex engineering rock mass is often simplified, which results in a certain deviation between the model and the real rock mass, and some difficulties are encountered in the selection of material parameters and the determination of constitutive relations, so the reliability of this method is often questioned; laboratory tests become the main means to verify the results of numerical simulation. At present, laboratory tests are becoming more and more important, but making samples with internal three-dimensional defects and complex geological structures is always one of the main restrictions on the development of rock mechanics tests. Preexisting fissures are always used to make samples, and there are two ways; one is to use tools (such as milling cutter, wire saw, and high-pressure water jet) to directly cut to obtain cracks in the rock cores [30–32]. However, due to the limitation of digging tools and the difference of mechanical properties caused by the complex microstructure inside the rock, the test data are often discrete. The other is directly casting samples containing preexisting fissures through similar rock materials such as gypsum and concrete [30, 33–35], but the roughness and the small opening of cracks are hardly guaranteed.

With the rise and progress of 3D printing technology, it is gradually possible to model entities with complex structures. 3D printing has the advantages of "any material, any part, any quantity, any location, and any field [36]," and it has been paid more attention and applied by rock mechanics researchers in recent years. Xiong et al. [37] made a number of rock samples with the same structure plane morphology using 3D printing technology and carried out a series of direct shear tests. The test results show that the values are consistent, and the dispersion of test results is small. Wang et al. [38] introduced a method of preparing fracture network models with different geometric shapes by 3D printing technology and carried out uniaxial compression laboratory tests for the RDFN model, linear DFN model, and solid model of rough fractured rock mass with different sample sizes. They found that the elastic modulus and uniaxial compressive strength of rock mass with preset fractures are significantly lower than those of solid rock model under uniaxial compression. The elastic modulus and uniaxial compressive strength of the RDFN model considering fracture roughness are higher than those of the linear DFN model. Without considering the roughness of joints, the compressive resistance of fractured rock mass will be underestimated. Zhao et al. [39] made parallel, combined, t-shaped, oblique, and orthogonal fracture models by 3D printing technology, poured rock-like samples containing different shapes of filling fractures with molds, and studied the variation rules of gas permeability of samples with different permeability structures under different confining pressures. These studies show that 3D printing technology overcomes the shortcomings of traditional specimen preparation methods and greatly improves the precision of fissure inserts, and an effective approach of solid complex structures reconstruction by 3D printing technology can be provided for indoor tests on the mechanical behavior of fractured rock mass.

In this paper, two basic parameters, roughness and gap width, are taken into account to conduct experimental research on seepage characteristics of through-filling fractured rock-like material based on 3D printing technology. The standard profile curves of 10 levels joint roughness (JRC = 0~20) proposed by Barton et al. [40, 41] are digitized to establish 10 groups of 3D digital fracture models with different roughness and thickness (1.5, 3.0, and 5.0 mm). Fracture inserts are produced by 3D printing technology to pour rock-like specimens with different roughness and gap widths. The permeability tests of the prepared rock-like specimens are carried out to study the seepage

characteristics of fractures with different roughness and gap widths under different confining pressures.

2. Specimen Production Based on 3D Printing Technology

2.1. 3D Printing of Fracture Inserts with Different Roughness and Thickness. The type of 3D printer used in the experiment is XYZPrinting DaVinci 3.0 (Figure 1), the printer's nozzle diameter is 0.4 mm, and the printing accuracy is 0.1 mm. The maximum size of the printable model is 200 mm × 200 mm×190 mm (length × width × height). The way of printing is melting accumulation, and the material used is PLA (poly lactic acid) polymer plastic. The sample is made by layering and melting stacking, and the thickness of printing layer is 0.3 mm.

The steps of making fracture inserts with different roughness and thickness are as follows. Firstly, based on Barton's standard profile curves of 10 grades of joint roughness, AutoCAD software is used to identify and reconstruct the roughness curve image, and 10 roughness curve models with a length of 10.0 cm were obtained, as shown in Figure 2(a). Secondly, 3D models of different JRC digitized joint surfaces were established by stretching in AutoCAD software (Figure 2(b)); Then, STL format files of each crack model are exported by AutoCAD software and imported in 3D printing software. As the model has a certain thickness, filling parameters need to be set. In order to ensure efficiency, the model is filled by interlacing with a thickness of 0.2 mm for each accumulation. The final printed inserts with different JRC joints are shown in Figure 2(c). As the model is established by melt accumulation method, the accumulation boundary of each layer is significant, and the printing models are uniform on the whole. Finally, 10 groups of 30 fracture inserts with different roughness and thickness of 1.5, 3.0, and 5.0 mm are produced, as shown in Figure 3.

2.2. Specimen Making. The rock-like material of specimens is made of cement mortar, and the material of through-filling cracks is made of gypsum mortar. Referring to the research of Li et al. [42, 43] and passing various proportioning tests, the rock-like material is mixed according to the mass ratio of ordinary Portland cement 42.5, river sand, gypsum, and water as 1 : 0.4 : 0.13 : 0.3, the permeability of the cement mortar samples without side pressure is $1.2 \times 10^{-18}\,m^2$, and the uniaxial compressive strength is 25 MPa. Compared with cement mortar, gypsum mortar has strong water permeability and high porosity, as well as certain strength and compressibility. It is better to simulate through-filling cracks. The gypsum mortar is mixed by the mass ratio of gypsum, river sand, and water as 1 : 0.8 : 0.6, the permeability of the gypsum mortar samples without side pressure is $3.8 \times 10^{-13}\,m^2$, and the uniaxial compressive strength is 4.6 MPa.

After the fissure inserts were made by 3D printer, the inserts were placed at the center of the molds, and the cement mortar was poured into the model after mixed evenly. During the pouring process, make sure that the crack insert piece is located in the center of the mold. After curing for 72 h, the inserts were removed and gypsum mortar was poured into the crack and fully filled. Molds were removed the next day and dried at normal temperature for 30 d to complete the specimens.

Thirty rock-like specimens with through-filling fractures including 10 grades roughness (JRC = 0~20) and three gap widths (1.5 mm, 3.0 mm, and 5.0 mm, respectively) have been produced; some specimens are shown in Figure 4.

3. Seepage Experiment of Fractured Rock-Like Samples

3.1. Experiment Scheme. Microcomputer controlled rock servo of triaxial test TAW2000 is used for penetrant test. The triaxial pressure chamber in the confining pressure system is reformed, the pressure chamber seat is replaced, and pore water is introduced into the pressure chamber to carry out the permeability test, rheological test, and stress-seepage coupling test. Three independent loading systems of axial pressure, confining pressure, and pore water pressure are equipped for the machine, which can apply the maximum confining pressure of 70 MPa, the maximum axial deviating stress of 500 MPa, and the maximum pore water pressure of 70 MPa. Axial and radial displacements are measured by the LVDT displacement sensor and chain extension meter, respectively.

The steady-state method is used in the test, and the permeable water pressure is applied at the bottom of the rock specimen through the stainless steel permeable pad at the lower end of the triaxial pressure chamber. Atmospheric pressure is maintained at the top of the specimen so that the osmotic pressure difference is formed at both ends of the specimen (see Figure 5). Changes in head pressure are recorded by a preset pressure sensor. A flow meter is set up at the seepage outlet at the other end of the pressure chamber to record the variation of seepage flow. According to Darcy's law, the calculation formula of rock specimen permeability is deduced as

$$k = \frac{\mu L Q}{A \Delta p \Delta t}, \tag{1}$$

where μ is hydrodynamic viscosity of water (it is 1.005×10^{-3}(Pa·s) at normal temperature); L is the length of the rock specimen (m); Q is seepage discharge; A is the cross-sectional area of rock specimen (m^2); and Δp is the difference of osmotic pressure between two ends of rock specimen (Pa).

During the test, only confining pressure and osmotic water pressure are applied, and no axial load is applied; the inlet water pressure was maintained at 1.0 MPa, and the outlet pressure is atmospheric pressure. The confining pressure changes with time, and the confining pressure is guaranteed to be larger than the osmotic water pressure in the same test. According to the purpose of the test, 8 values of confining pressure are selected: 1.2, 1.4, 1.6, 2.0, 3.0, 5.0, 8.0, and 12.0 MPa, respectively. At the same time, in order to fully reflect the percolation characteristics of the specimens

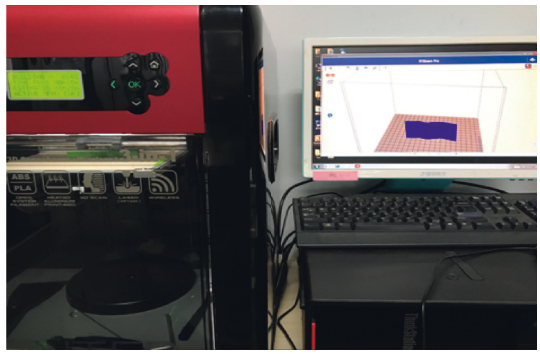

Figure 1: XYZPrinting DaVinci 3D printing system.

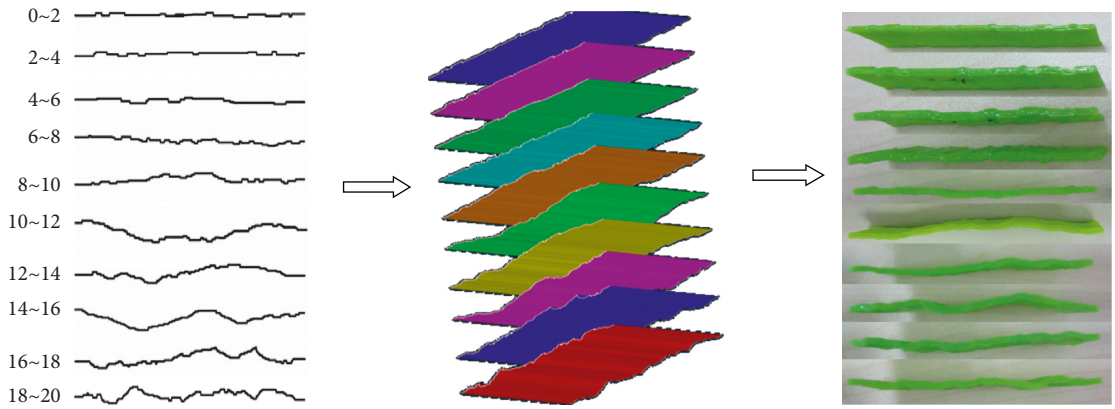

Figure 2: Barton's curves with varied JRC values and corresponding 3D models: (a) Barton's 10 JRC curves; (b) 3D stretch JRC surface; (c) 1.5 mm print solid model.

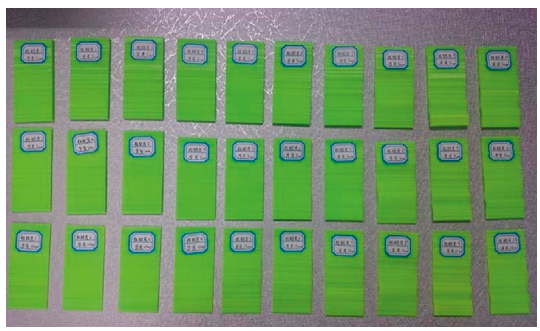

Figure 3: Fracture inserts with different roughness and thickness.

Figure 4: Part of the specimens: (a) three kinds of gap widths when JRC is 5; (b) three kinds of gap widths when JRC is 9.

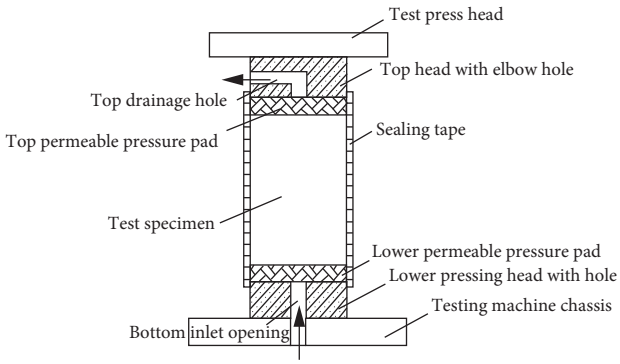

Figure 5: Test device and principle.

under the condition of water saturation, the prepared specimens are firstly tested with vacuum water saturation and soaked in distilled water for 48 h before the test. During the test, the steady seepage discharges of the specimens under different confining pressures are recorded by the flow meter and the permeability is calculated.

3.2. Test Results and Analysis

3.2.1. Influence of Confining Pressure on Permeability of Through-Filling Fractures. The relations between confining pressure and permeability of through-filling fracture with different roughness and gap widths are shown in Figure 6. As shown in the figure, the permeability of the through-filling fractures with different roughness and gap width decreases with the increase of confining pressure, and at the initial stage of confining pressure loading (1.2~3.0 MPa), the fracture permeability decreases rapidly. However, in the middle and later stage of loading (3.0~12.0 MPa), the decrease rate of fracture permeability is relatively slow. The reason is that the pore structure of filling medium inside the fracture is the main seepage channel in the early stage of loading, and with the increase of confining pressure, the gap between fractures decreases and the porosity of the filling medium reduces. In the middle and later periods of the confining pressure loading, irreversible plastic deformation occurs because the filling medium of fracture has been compacted at the early stage of loading and theirspace structure is destroyed, the rest of the seepage channel is closed down. At this time, the increase of confining pressure has a small effect on fracture seepage channel, and then the rate of permeability declines to slow down.

After the permeability test, it was found that the gypsum mortar in the through-filling fracture of each specimen has been compacted, concave holes appear in the gypsum mortar at the top of the specimen (which is the outlet of pore water) fillin. When the gap width is bigger (i.e., 3 mm and 5 mm), there are obvious holes and seepage channels formed by vertical cracks on the surface of filling gypsum mortar, which indicates that plastic failure occurred in the interior of gypsum mortar, and the filling gypsum mortar tend to extrude from cracks.

3.2.2. Effect of Roughness on Permeability of Through-Filling Fractures. According to Figure 6(a), when the gap width is 1.5 mm, at the initial stage of confining pressure loading, the fracture permeability at the same confining pressure tends to decrease with the increase of roughness, and the dispersion is relatively large. With the increase of confining pressure, this trend gradually weakens, and the influence of roughness on the permeability of through-filling fracture decreases gradually. The reason may be that in the early stage of confining pressure loading, the pore structures in the thin layer of filling media with different roughness curves have not been compacted yet, which constitutes the main seepage channel through the filling fracture. In this case, the roughness has a strong influence on the permeability of the fracture; the larger the value is, the longer the seepage path will be and the lower the permeability of the through-filling fracture will be. In the middle and later periods of the confining pressure loading, because the thin layer medium is pressured, even plastic failed (when confining pressure is greater than the compressive strength of gypsum mortar), the porosity decreases rapidly and flow capacity reduces, and the influence of seepage path on the permeability of through-filling crack decreases, the enhanced influence of confining pressure leads to reduction of the difference of permeability of filling fractures with different roughness. With the increase of the gap width, the permeability dispersion of filling fractures with different roughness under the same confining pressure decreases significantly, and the influence of roughness on permeability decreases as shown in Figures 6(b) and 6(c).

This phenomenon can also be illustrated by the change of the permeability standard deviation of through-filling fractures with 10 grades roughness at every gap width under the same confining pressure (Figure 7). As shown in Figure 7, in the early stage of confining pressure loading, the larger the gap width is, the smaller the permeability standard deviation of the through-filling fracture with different roughness is. The reason is with the increase of the thickness of the fracture, the influence of the roughness coefficient of the fracture surface (effective height) on the seepage path of the filling fracture will be gradually weakened. When the filling thickness is large enough, the influence of fracture surface roughness will be completely eliminated. When the gap width is 5.0 mm, the permeability standard deviation of the filling fracture with different roughness is basically unchanged during confining pressure loading. In addition, with the increase of confining pressure, the permeability standard deviation of the filling fracture with different roughness and widths of 1.5 mm and 3.0 mm decreases rapidly and tends to be stable.

3.2.3. Effect of Gap Width on Permeability of Through-Filling Fractures. The influence of gap width on permeability of through-filling fractures is shown in Figure 8. For through-filling fractures with different roughness, there is a rule that the larger the gap width is, the greater the fracture permeability is at the beginning and the end of confining pressure loading. The reason is that the filling medium in the

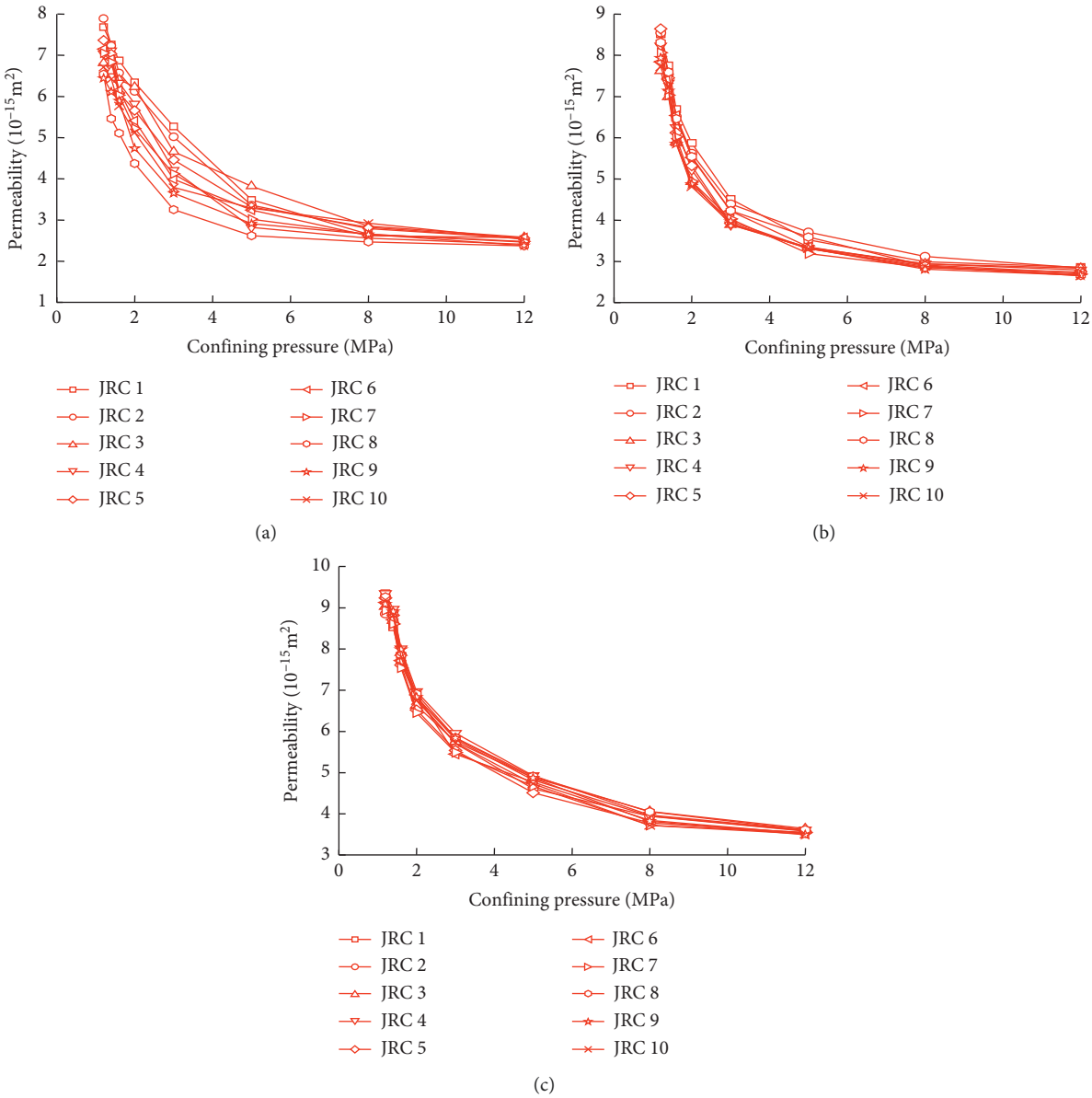

Figure 6: Relations between confining pressure and permeability of through-filling fractures with different JRCs and gap widths: (a) gap width 1.5 mm; (b) gap width 3.0 mm; (c) gap width 5 mm.

fractures has high porosity and strong permeability, and if roughness of fractures is the same, the larger the filling medium thickness (equal to the gap width) is, the larger the cross-sectional area of the seepage flow will be, which leads to a higher fracture permeability. Meanwhile, in the process of confining pressure loading, the permeability curves of the through-filling fractures with gap widths of 1.5 mm and 3.0 mm are intersected twice. The reason may be that in the early stage of the confining pressure loading, pore structures in the through-filling medium are compressed both at the gap widths of 1.5 mm and 3.0 mm, but relative to the through-filling fracture with gap width of 1.5 mm, the range of pore structure is bigger, the compression amount is larger at gap width 3.0 mm, and the permeability declines faster. Thus, the permeability curves at two gap widths are crossed for the first time. With the continuous increase of confining pressure, the pore structure of the filling medium in the fracture with gap widths of 1.5 mm and 3.0 mm is gradually compacted and the permeability gradually tends to be stable. At this moment, the seepage cross-sectional area at the gap width of 3.0 mm is larger than that of 1.5 mm and the permeability decreases slowly and leads to the second crossover in the permeability curve between the gap widths of 1.5 mm and 3.0 mm.

As shown in Figure 8, the confining pressure-permeability test results of through-filling fractures with different roughness and gap widths can be described by the following functional relationship by nonlinear fitting:

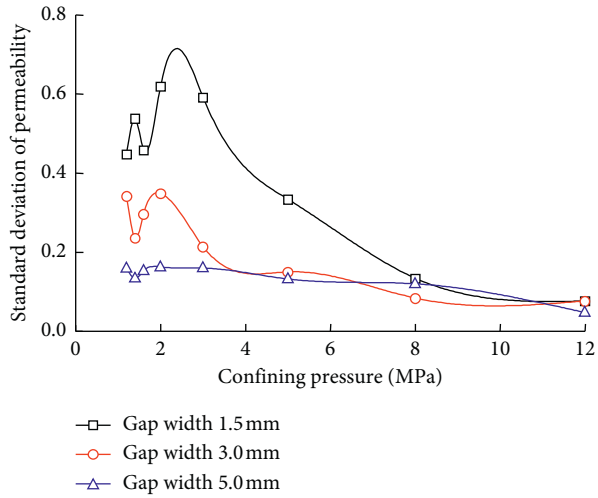

Figure 7: Relationship between permeability standard deviation of through-filling fractures with different JRCs and confining pressures.

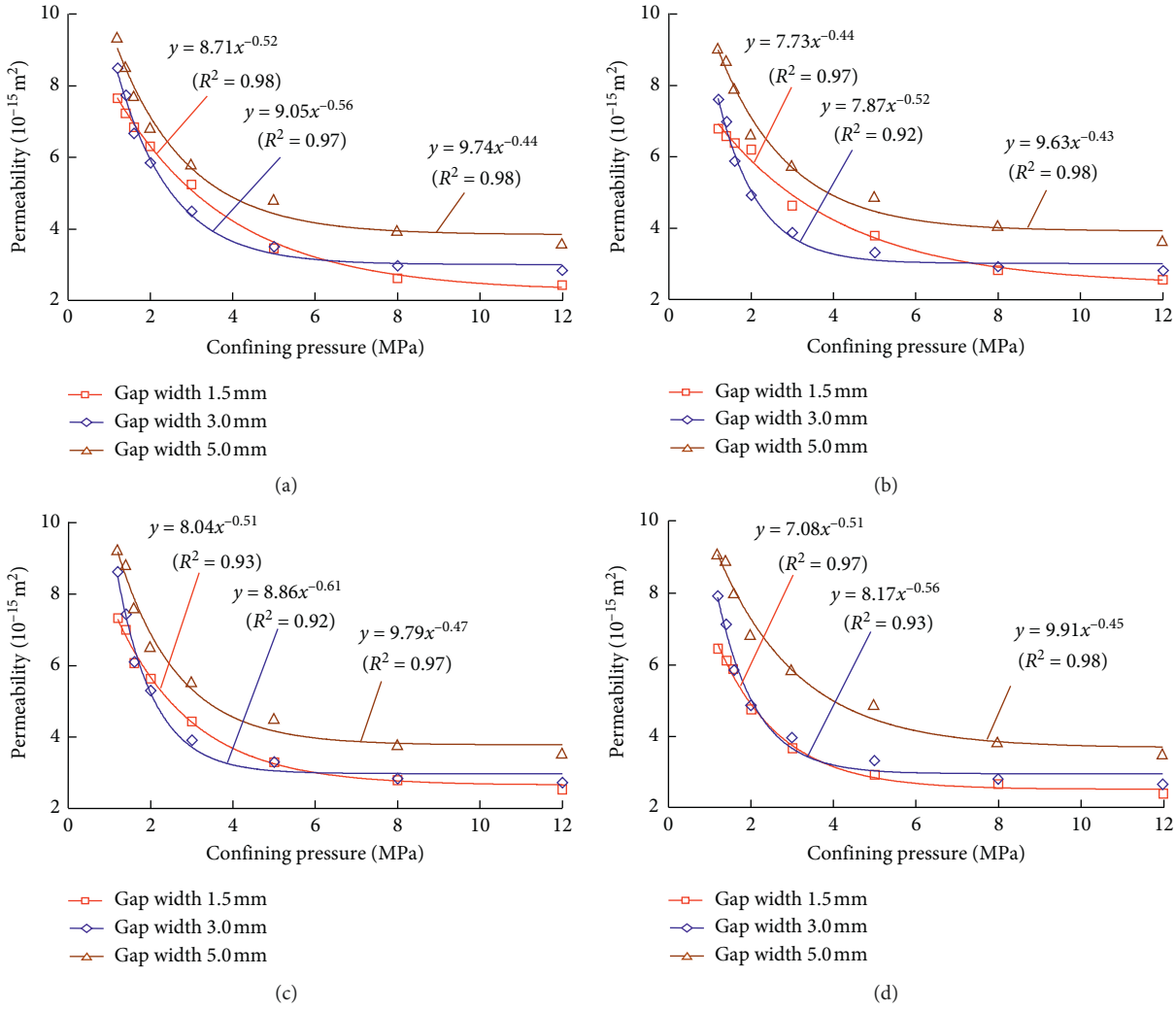

Figure 8: Results of confining pressure versus permeability of through-filling fracture with different gap widths: (a) JRC = 1; (b) JRC = 3; (c) JRC = 5; (d) JRC = 9.

Table 1: Initial permeability k_0 and fitting parameter α at different roughness and gap widths.

The rank of JRC	Gap width 1.5 mm		Gap width 3.0 mm		Gap width 5.0 mm	
	k_0	α	k_0	α	k_0	α
1	8.71	0.52	9.05	1	8.71	0.52
2	7.24	0.47	8.08	2	7.24	0.47
3	7.73	0.44	7.87	3	7.73	0.44
4	8.18	0.56	8.55	4	8.18	0.56
5	8.04	0.51	8.86	5	8.04	0.51
6	7.91	0.53	8.52	6	7.91	0.53
7	7.83	0.53	8.27	7	7.83	0.53
8	6.64	0.53	8.82	8	6.64	0.53
9	7.08	0.51	8.17	9	7.08	0.51
10	7.24	0.47	8.08	10	7.24	0.47

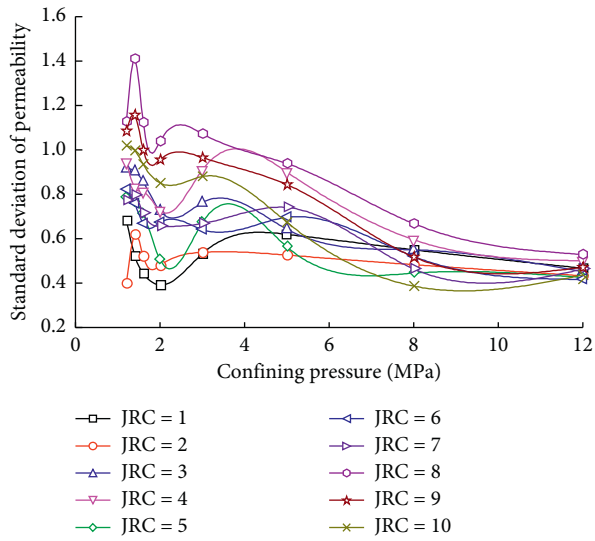

Figure 9: Relationship between permeability standard deviation of through-filling fractures with different gap widths and confining pressures.

$$k = k_0 p_c^{-\alpha}, \tag{2}$$

where k is the permeability of fractures (m^2); k_0 is the initial permeability (m^2); α is a fitting parameters; and p_c is the confining pressure (MPa). Initial permeability k_0 and fitting parameter α at different roughness and gap widths can be seen in Table 1.

The fitting degrees of the curves are all higher than 95.92%, so the fitting effect is very good. Thus, this function can be used to describe the confining pressure-permeability relationship of the through-filling fractures with different roughness and gap widths.

Figure 9 shows the variation rule of the permeability standard deviation of three gap widths at 10 grades roughness under confining pressure. As shown in Figure 9, in the early stage of confining pressure loading, the permeability standard deviation of through-filling fractures tends to increase with the increase of roughness and confining pressures. However, with the increase of confining pressure, the permeability standard deviation of through-filling fractures with different roughness decreased and the influence of roughness on the permeability of the through-filling fractures will be gradually eliminated.

4. Conclusion

Based on 3D digital modeling and 3D printing technology, 30 rock specimens with 10 grades roughness (JRC = 0~20) and 3 kinds of gap width (1.5, 3.0, and 5.0 mm respectively) were produced, and permeability tests were carried out within the range of permeability pressure 1.0 MPa and confining pressure 1.2~12.0 MPa; the conclusions are as follows:

(1) Combined with 3D digital reconstruction and 3D printing technology, fracture structures with different roughness and gap widths can be produced quickly by the method of preexisting fissures. Although 3D printing materials are not suitable as substitutes for natural rock materials at present, due to the disadvantages of low strength and high plasticity, it can greatly improve the precision of fracture inserts and be helpful for test model preparation of complex fractured rock mass.

(2) Roughness and gap width are important factors affecting the seepage characteristics of jointed rock mass. When the gap width is relatively small (1.5 mm), the effect of roughness on the permeability of the through-filling fracture is obvious at the initial stage of confining pressure loading, and the fracture permeability decreases with the increase of roughness. With the increase of confining pressure and gap width, the effect of roughness on fracture permeability decreases rapidly.

(3) The permeability of through-filling fractures with different roughness and gap widths decreases with the increase of confining pressure. In the early stage of confining pressure loading, the rate of permeability of fractures decreases rapidly, and in the middle and later stages of confining pressure loading, the rate of permeability decreases rapidly.

(4) In the process of confining pressure loading, there is a rule that the greater the gap width is, the greater the crack permeability is when the confining pressure is small. The greater the roughness is, the greater the difference of the permeability between different gap widths is. However, with the increase of confining pressure, the effect of roughness will be gradually eliminated. The relationship between confining pressure and permeability of through-filling fracture can be described by the power function.

Data Availability

The data used to support the findings of this study are available from the corresponding author upon request.

Conflicts of Interest

The authors declare that they have no conflicts of interest.

Acknowledgments

This study was supported by the State Key Research Development Program of China (grant no. 2017YFC0804103) and the National Natural Science Foundation of China (grant no. 11572344).

References

[1] D. T. Snow, "Anisotropic permeability of fractured media," *Water Resource Research*, vol. 5, no. 6, pp. 1273–1289, 1969.

[2] D. T. Snow, *A Parallel Plate Model of Fractured Permeable Media*, University of California, Oakland, CA, USA, 1976.

[3] E. S. Romm, *Flow Characteristics of Fractured Rocks*, Nedra, Moscow, Russia, 1966.

[4] C. Louis, *A Study of Groundwater Flow in Jointed Rock and its Influence on the Stability of Rock Masses*, Imperial College, London, UK, 1969.

[5] C. Louis, *Rock Hydraulics in Rock Mechanics*, Elsevier Science, New York, NY, USA, 1974.

[6] B. Amadei and T. Illangasekare, "A mathematical model for flow and solute transport in non-homogeneous rock fracture," *International Journal of Rock Mechanics and Mining Sciences & Geomechanics Abstracts*, vol. 31, no. 6, pp. 719–731, 1994.

[7] B. Y. Su, M. L. Zhan, and J. Zhao, "Study on fracture seepage in the imitative nature rock," *Chinese Journal of Geotechnical Engineering*, vol. 15, no. 7, pp. 19–24, 1995, in Chinese.

[8] W. Zhu and T.-F. Wong, "The transition from brittle faulting to cataclastic flow: permeability evolution," *Journal of Geophysical Research: Solid Earth*, vol. 102, no. B2, pp. 3027–3041, 1997.

[9] B. P. Han, Q. Y. Feng, L. S. Yu et al., "Study on permeability of carbonate rocks during full stress-strain process," *Journal of Engineering Geology*, vol. 8, no. 2, pp. 127-128, 2000, in Chinese.

[10] O. Schulze, T. Popp, and H. Kern, "Development of damage and permeability in deforming rock salt," *Engineering Geology*, vol. 61, no. 2-3, pp. 163–180, 2001.

[11] M. Oda, T. Takemura, and T. Aoki, "Damage growth and permeability change in triaxial compression tests of Inada granite," *Mechanics of Materials*, vol. 34, no. 2, pp. 313–331, 2002.

[12] J. A. Wang and H. D. Park, "Fluid permeability of sedimentary rocks in a complete stress-strain process," *Engineering Geology*, vol. 63, no. 3-4, pp. 291–300, 2002.

[13] J. B. Yang, X. T. Feng, and P. Z. Pang, "Experimental study of permeability characteristics of single rock fracture considering stress history," *Rock and Soil Mechanics*, vol. 34, no. 6, pp. 1629–1635, 2013, in Chinese.

[14] L. M. Yin, G. Wang, W. B. Sun et al., "Experimental study of effect of joint roughness on stress-seepage coupling characteristics," *Journal of Shandong University of Science and Technology*, vol. 31, no. 6, pp. 30–35, 2012, in Chinese.

[15] M. B. Duan, G. Li, Y. F. Meng et al., "Research on regulation of fracture seepage in different joint roughness coefficients," *Journal of Water Resources & Water Engineering*, vol. 24, no. 5, pp. 41–44, 2013, in Chinese.

[16] R. W. Zimmerman, A. Al-Yaarubi, C. C. Pain, and C. A. Grattoni, "Nonlinear regimes of fluid flow in rock fractures," *International Journal of Rock Mechanics and Mining Sciences*, vol. 41, no. 3, pp. 163–169, 2004.

[17] M. Zoorabadi, S. Saydam, W. Timms, and B. Hebblewhite, "Non-linear flow behavior of rough fractures having standard JRC profiles," *International Journal of Rock Mechanics and Mining Sciences*, vol. 76, pp. 192–199, 2015.

[18] C. B. Zhou, Z. T. Ye, and B. Han, "A study on configuration and hydraulic conductivity of rock joints," *Advances in Water Science*, vol. 8, no. 3, pp. 233–239, 1997, in Chinese.

[19] R. C. Liu, Y. J. Jiang, B. Li et al., "Nonlinear seepage behaviors of fluid in fracture networks," *Rock and Soil Mechanics*, vol. 37, no. 10, pp. 2817–2824, 2016, in Chinese.

[20] R. Liu, B. Li, and Y. Jiang, "A fractal model based on a new governing equation of fluid flow in fractures for characterizing hydraulic properties of rock fracture networks," *Computers and Geotechnics*, vol. 75, pp. 57–68, 2016.

[21] Q. S. Liu, Y. X. Wu, and X. Y. Liu, "Computer simulation of 2D rough joint network," in *Proceedings of the 2nd Conference of Underground Waste Disposal, Chinese Society for Rock Mechanics and Engineering*, pp. 91–96, 2008, in Chinese.

[22] Y. X. Wu, *Modelling Rough Joint Network and Study on Hydro-Mechanical Behavior of Fractured Rock Mass*, Institute of Rock and Soil Mechanics, Chinese Academy of Sciences, Wuhan, China, 2010, in Chinese.

[23] Z. Zhao, B. Li, and Y. Jiang, "Effects of fracture surface roughness on macroscopic fluid flow and solute transport in fracture networks," *Rock Mechanics and Rock Engineering*, vol. 47, no. 6, pp. 2279–2286, 2014.

[24] K.-B. Min, L. Jing, and O. Stephansson, "Determining the equivalent permeability tensor for fractured rock masses using a stochastic REV approach: method and application to the field data from Sellafield, UK," *Hydrogeology Journal*, vol. 12, no. 5, pp. 497–510, 2004.

[25] A. Baghbanan and L. Jing, "Hydraulic properties of fractured rock masses with correlated fracture length and aperture," *International Journal of Rock Mechanics and Mining Sciences*, vol. 44, no. 5, pp. 704–719, 2007.

[26] Y. Wang and B. Y. Su, "Seepage characteristic of single fracture plane and equivalent hydraulic width," *Advances in Water Science*, vol. 13, no. 1, pp. 61–68, 2002.

[27] Y. Wang, "Coupling characteristic of seepage and stress of single fracture plane," *Chinese Journal of Rock Mechanics and Engineering*, vol. 21, no. 1, pp. 83–87, 2002.

[28] X. B. Xiong, C. H. Zhang, and E. Z. Wang, "A review of steady state seepage in a single fracture of rock," *Chinese Journal of Rock Mechanics and Engineering*, vol. 28, no. 9, pp. 1839–1846, 2009.

[29] Y. L. He, Y. J. Tao, and L. Z. Yang, "Experimental research on hydraulic behaviors in a single joint with various values of JRC," *Chinese Journal of Rock Mechanics and Engineering*, vol. 29, no. 1, pp. 3235–3240, 2010.

[30] L. N. Y. Wong and H. H. Einstein, "Systematic evaluation of cracking behavior in specimens containing single flaws under uniaxial compression," *International Journal of Rock Mechanics and Mining Sciences*, vol. 46, no. 2, pp. 239–249, 2009.

[31] S.-Q. Yang, H.-W. Jing, and T. Xu, "Mechanical behavior and failure analysis of brittle sandstone specimens containing combined flaws under uniaxial compression," *Journal of Central South University*, vol. 21, no. 5, pp. 2059–2073, 2014, in Chinese.

[32] S. Q. Yang, Y. H. Dai, L. J. Han et al., "Uniaxial compression experimental research on deformation and failure properties of brittle marble specimen with pre-existing fissures," *Chinese*

Journal of Rock Mechanics and Engineering, vol. 28, no. 12, pp. 2391–2404, 2009, in Chinese.

[33] R. H. C. Wong, P. Lin, C. A. Tang et al., "Mechanisms of crack coal essence of pre-existing flaws under biaxial compression," *Chinese Journal of Rock Mechanics and Engineering*, vol. 21, no. 6, pp. 808–816, 2002, in Chinese.

[34] D. L. Grote, S. W. Park, and M. Zhou, "Dynamic behavior of concrete at high strain rates and pressures: I. Experimental characterization," *International Journal of Impact Engineering*, vol. 25, no. 9, pp. 869–886, 2001.

[35] A. V. Dyskin, E. Sahouryeh, R. J. Jewell, H. Joer, and K. B. Ustinov, "Influence of shape and locations of initial 3D cracks on their growth in uniaxial compression," *Engineering Fracture Mechanics*, vol. 70, no. 15, pp. 2115–2136, 2003.

[36] B. Lu, D. Li, and X. Tian, "Development trends in additive manufacturing and 3D printing," *Engineering*, vol. 1, no. 1, pp. 085–089, 2015.

[37] Z. Q. Xiong, Q. Jiang, Y. H. Gong et al., "Modeling natural joint of rock mass using three dimensional scanning and printing technologies and its experimental verification," *Rock and Soil Mechanics*, vol. 36, no. 6, pp. 1557–1565, 2015, in Chinese.

[38] P. T. Wang, Y. Liu, L. Zhang et al., "Preliminary experimental study on uniaxial compressive properties of 3D printed fractured rock models," *Chinese Journal of Rock Mechanics and Engineering*, vol. 37, no. 2, pp. 364–373, 2018, in Chinese.

[39] K. Zhao, H. L. Wang, W. Y. Xu et al., "Experimental study on seepage characteristics of rock-like materials with consecutive and filling fractures," *Chinese Journal of Geotechnical Engineering*, vol. 39, no. 6, pp. 1130–1136, 2017, in Chinese.

[40] W. Tian and N. Han, "Preliminary research on mechanical properties of 3D printed rock structures," *Geotechnical Testing Journal*, vol. 40, no. 3, pp. 483–493, 2017.

[41] M. C. He, H. P. Xie, S. P. Peng et al., "Study on rock mechanics in deep mining engineering," *Chinese Journal of Rock Mechanics and Engineering*, vol. 34, no. 11, pp. 2161–2178, 2015, in Chinese.

[42] X. H. Li, Y. Y. Lu, Y. Kang et al., *Rock Mechanics Experiment Simulation Technology*, Science Press, Beijing, China, 2007, in Chinese.

[43] X. Y. Liu, A. H. Liu, and X. B. Li, "Experimental study of permeability of rock-like material with filling fractures under high confining pressure," *Chinese Journal of Rock Mechanics and Engineering*, vol. 31, no. 7, pp. 1390–1398, 2012, in Chinese.